2022/10/14

星形成ゼミ
The Star Formation Newsletter 354
36~42

徳田一起 (九州大学/国立天文台)

36	The Role of Magnetic Fields in the Stability and Fragmentation of Filamentary Molecular Clouds: Two Case Studies at OMC-3 and OMC-4
37	A massive Keplerian protostellar disk with flyby-induced spirals in the Central Molecular Zone
38	Gaia EDR3 comparative study of protoplanetary disk fractions in young stellar clusters
39	Gas Column Density Distribution of Molecular Clouds in the Third Quadrant of the Milky Way
40	Modeling snowline locations in protostars: The impact of the structure of protostellar cloud cores
41	ALMA Images the Eccentric HD 53143 Debris Disk
42	Unraveling the observational signatures of cloud-cloud collision and hub-filament sys- tems in W31

36 **The Role of Magnetic Fields in the Stability and Fragmentation of Filamentary Molecular Clouds: Two Case Studies at OMC-3 and OMC-4**

Pak Shing Li, Enrique Lopez-Rodriguez, Archana Soam, Richard I. Klein ★ We present the stability analysis of two regions, OMC-3 and OMC-4, in the massive and long molecular cloud complex of Orion A. We obtained 214 μm HAWC+/SOFIA polarization data, and we make use of archival data for the column density and $C^{18}O$ (1-0) emission line. We find clear depolarization in both observed regions and that the polarization fraction is anti-correlated with the column density and the polarization-angle dispersion function. We find that the filamentary cloud and dense clumps in OMC-3 are magnetically supercritical and strongly subvirial. This region should be in the gravitational collapse phase and is consistent with many young stellar objects (YSOs) forming in the region. Our histogram of relative orientations (HROs) analysis shows that the magnetic field is dynamically sub-dominant in the dense gas structures of OMC-3. We present the first polarization map of OMC-4. We find that the observed region is generally magnetically subcritical except for an elongated dense core, which could be a result of projection effect of a filamentary structure aligned close to the line-of-sight. The relative large velocity dispersion and the unusual positive shape parameters at high column densities in the HROs analysis suggest that our viewing angle may be close to axes of filamentary substructures in OMC-4. The dominating strong magnetic field in OMC-4 is unfavorable for star formation and is consistent with much fewer YSOs than in OMC-3.

磁場(の相対的な働き)がOMC-3とOMC-4で違う

37 **A massive Keplerian protostellar disk with flyby-induced spirals in the Central Molecular Zone**

Xing Lu, Guang-Xing Li, Qizhou Zhang, Yuxin Lin ★ Accretion disks are an essential component in the paradigm of the formation of low-mass stars. Recent observations further identify disks surrounding low-mass pre-main-sequence stars perturbed by flybys. Whether disks around more massive stars evolve in a similar manner becomes an urgent question. We report the discovery of a Keplerian disk of a few solar masses surrounding a 32 solar-mass protostar in the Sagittarius C cloud around the Galactic Center. The disk is gravitationally stable with two embedded spirals. A combined analysis of analytical solutions and numerical simulations demonstrates that the most likely scenario to form the spirals is through external perturbations induced by a close flyby, and one such perturber with the expected parameters is identified. The massive, early O-type star embedded in this disk forms in a similar manner with respect to low-mass stars, in the sense of not only disk-mediated accretion, but also flyby-impacted disk evolution.

・銀河中心部のALMAの観測(大質量星周り)
・小質量星と同様なと同様に形成されるが、flybyによってスパイラルが誘起されるか？
=>ALMAのwebサイトでプレスリリース記事
https://alma-telescope.jp/news/accretiondisk-202206

サジタリウスC分子雲(銀河中心)に本当にあるのか？
-速度が同じ(-50 km/s)で分子輝線の線幅も円盤領域より大きい(>2km/s)

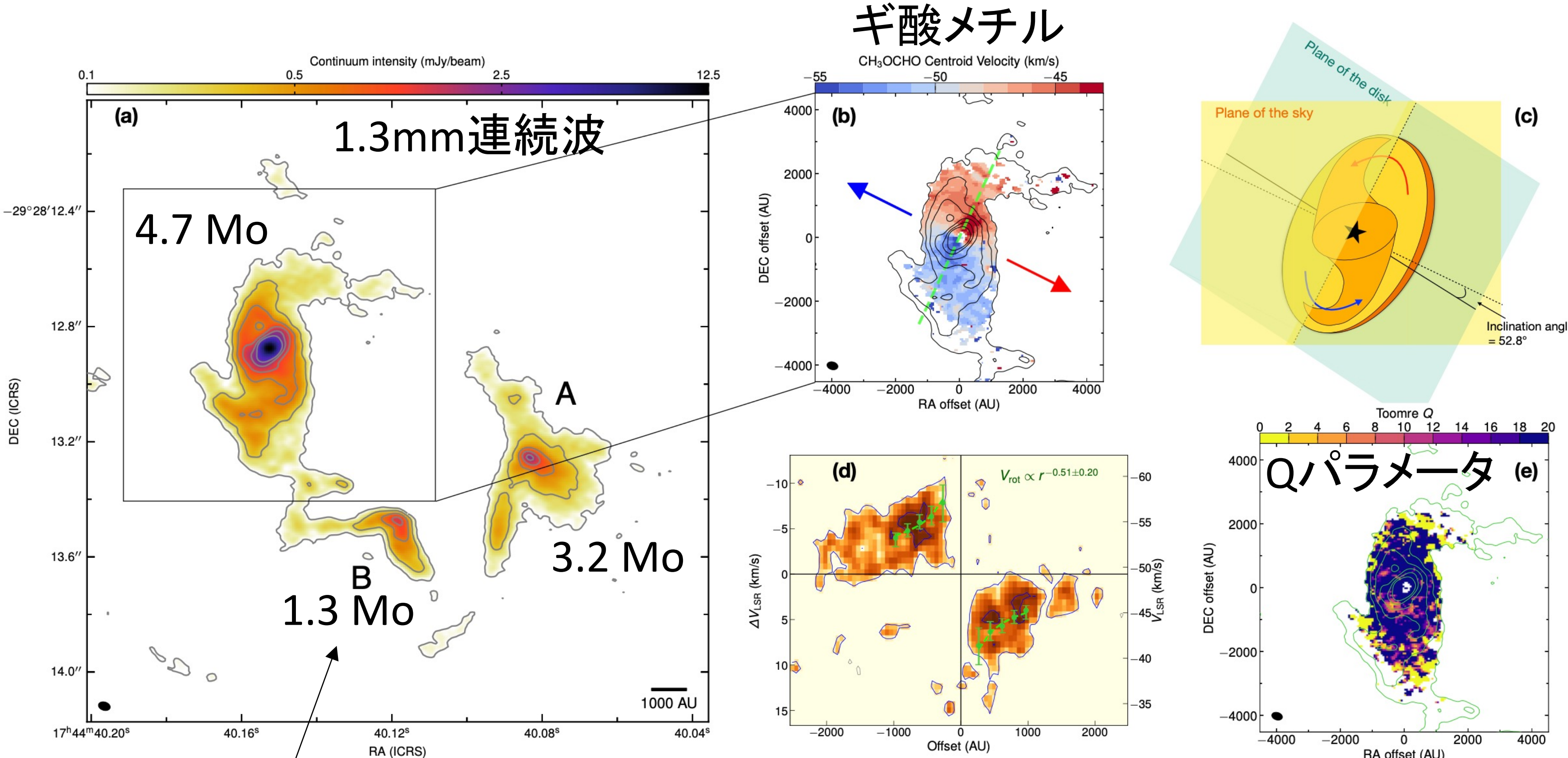

32 Mo中心星のケプラーfit　　円盤は安定?
中心星の明るさ ~ a few x 10^5 Lo

Bの影響はfly-byに考慮に入っていない(入れていない)

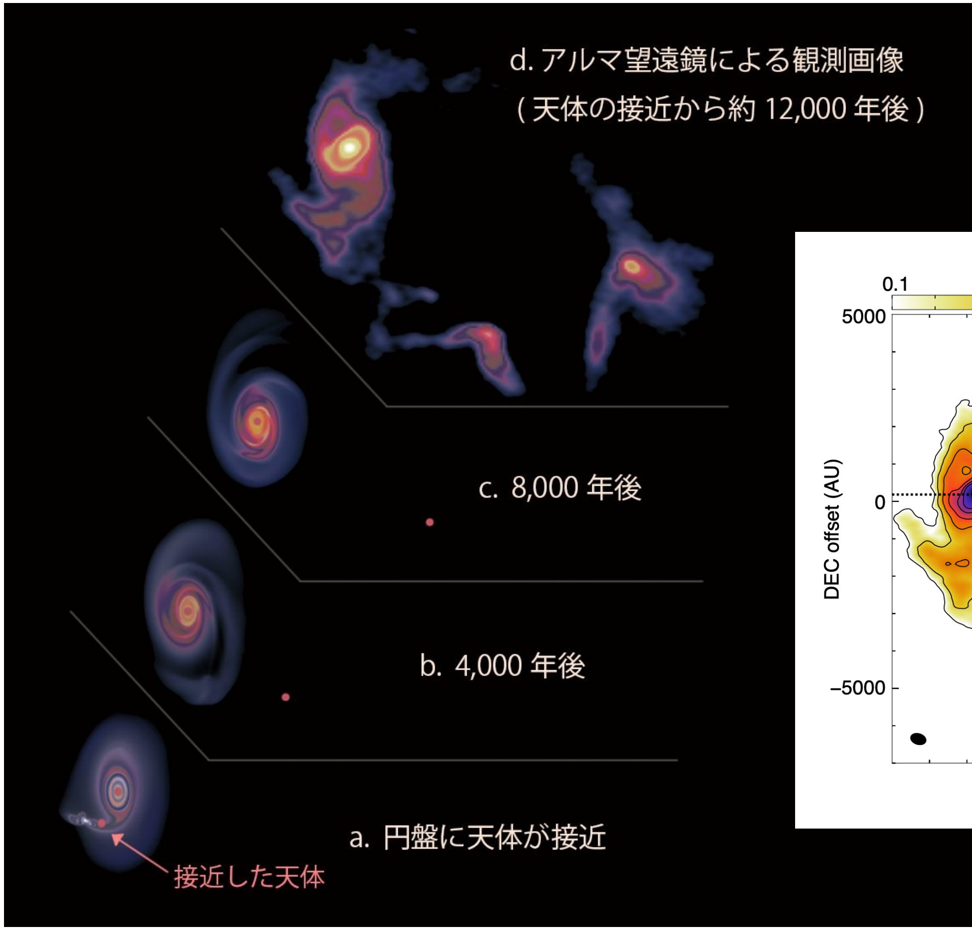

Credit: Lu et al.

流体計算コード
PHANTOMで計算

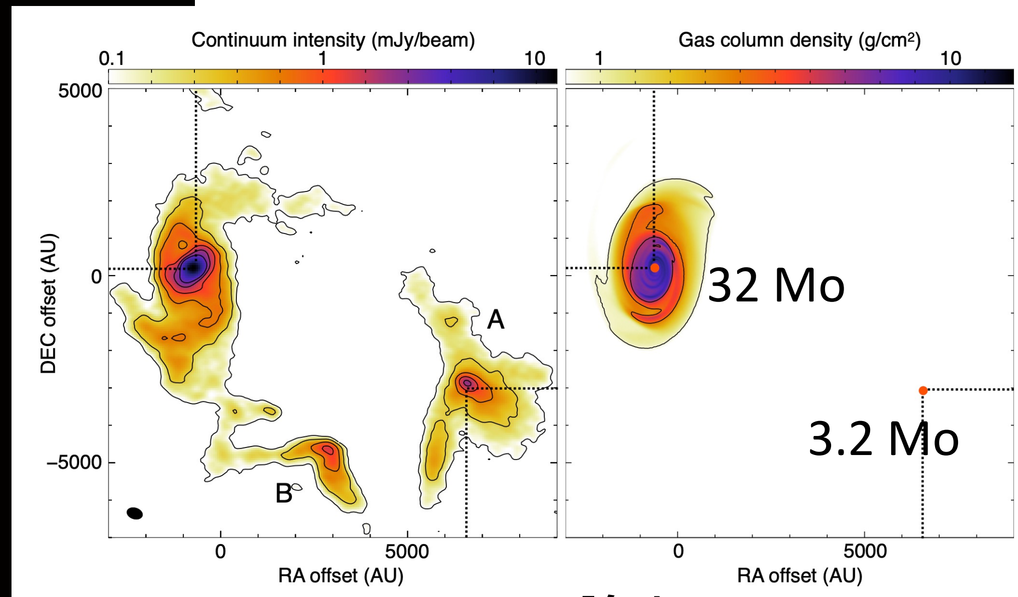

論文の図
赤点がsink 粒子

疑問: ソースAは3.2で本当に良いのか？

Fly-byイベントは起こりうるのか？

- サジタリウスCでの星の密度5 x 10^4 pc^-3

星の間の相対速度1km/s, 近点2000au, 相互作用する合計質量 40 Moの場合

タイムスケールは、800年になる

=>大質量星の原始星(円盤)が回転する時間及び、進化タイムスケール10^4 yrより十分短い

38 **Gaia EDR3 comparative study of protoplanetary disk fractions in young stellar clusters**

I. Mendigutía, E. Solano, M. Vioque, L. Balaguer-Nuñez, A. Ribas, N. Huélamo, C. Rodrigo ★ (Abridged) The lifetime of protoplanetary disks around young stars limits the timescale when planets form. A disk dissipation timescale < 10 Myr was inferred from surveys providing the fraction of stars with disks in young stellar clusters with different ages. However, most previous surveys focused on the compact region within 2 pc from the clusters' centers, for which the disk fraction information considering the outer part is practically absent. We aim to test if disk fraction estimates change when inferred from an extended region around the clusters' centers. Gaia EDR3 data and a best-suited, Virtual Observatory (VO)-based tool -Clusterix-, are used to identify member stars for a representative sample of 19 young clusters considering two concentric fields of view (FOV) with radii 20 pc and 2 pc. Our analysis reveals that the inner disk fractions inferred from the compact and the extended regions are equal within 10%, which does not support a previous hypothesis proposing that disk fractions should be significantly larger considering extended regions. A list of member and disk stars in each cluster is provided and stored in a VO-compliant archive. Averaged values and plots characterizing the whole clusters are also provided, including HR diagrams based on Gaia colors and absolute magnitudes. Our results cover the largest fields ever probed when dealing with disk fractions for all clusters analysed, and imply that their complete characterization requires the use of wide FOVs. The resulting database is a benchmark for future detailed studies of young clusters, whose disk fractions must be accurately determined by using multi-wavelength analysis potentially combined with data from coming Gaia releases.

39 **Gas Column Density Distribution of Molecular Clouds in the Third Quadrant of the Milky Way**

Yuehui Ma, Hongchi Wang, Miaomiao Zhang, Chen Wang, Shaobo Zhang, Yao Liu, Chong Li, Yuqing Zheng, Lixia Yuan, Ji Yang ★ We have obtained column density maps for an unbiased sample of 120 molecular clouds in the third quadrant of the Milky Way mid-plane (b$\leq |5|^\circ$) within the galactic longitude range from 195° to 225°, using the high sensitivity ^{12}CO and ^{13}CO ($J = 1-0$) data from the Milky Way Imaging Scroll Painting (MWISP) project. The probability density functions of the molecular hydrogen column density of the clouds, N-PDFs, are fitted with both log-normal (LN) function and log-normal plus power-law (LN+PL) function. The molecular clouds are classified into three categories according to their shapes of N-PDFs, i.e., LN, LN+PL, and UN (unclear), respectively. About 72% of the molecular clouds fall into the LN category, while 18% and 10% into the LN+PL and UN categories, respectively. A power-law scaling relation, $\sigma_s \propto N_{H_2}^{0.44}$, exists between the width of the N-PDF, σ_s, and the average column density, N_{H_2}, of the molecular clouds. However, σ_s shows no correlation with the mass of the clouds. A correlation is found between the dispersion of normalized column density, $\sigma_{N/<\mathrm{N}>}$, and the sonic Mach number, $\mathcal{M}$, of molecular clouds. Overall, as predicted by numerical simulations, the N-PDFs of the molecular clouds with active star formation activity tend to have N-PDFs with power-law high-density tails.

*距離が500 pc~10 kpcのものを全部一気に解析している点に注意

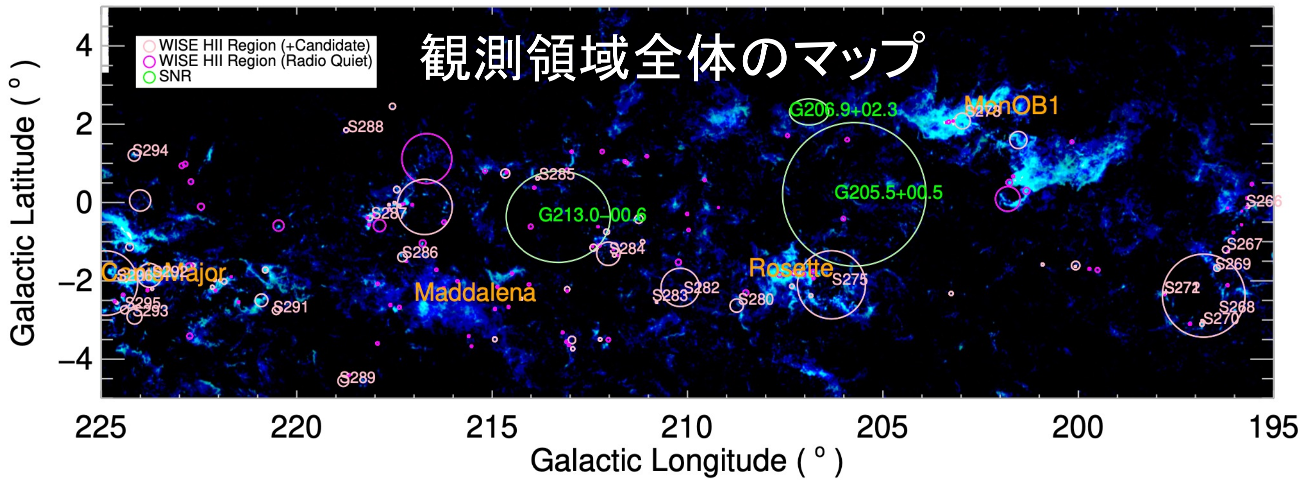

Figure 1. RGB map of the integrated intensity of the ^{12}CO , ^{13}CO , and C^{18}O $J = 1 - 0$ emission, T_{mb}. Red, green, and blue

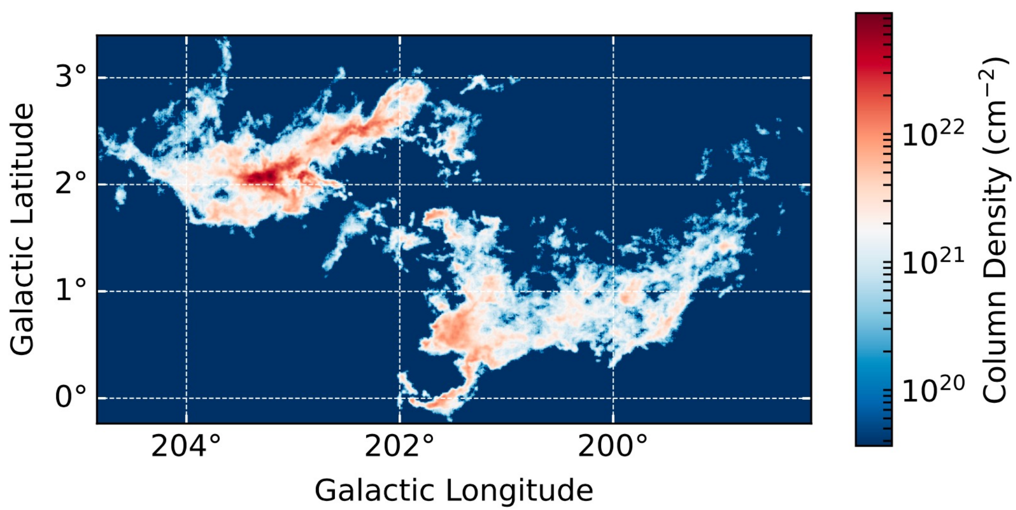

MonOB1領域のマップ

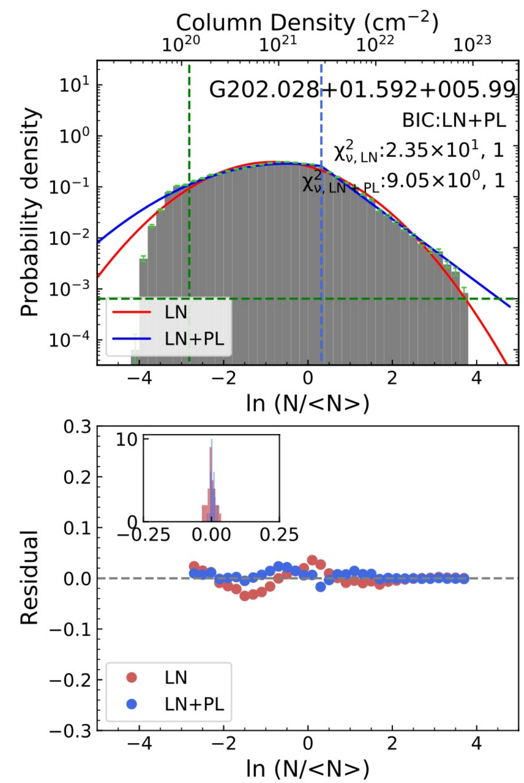

NPDFのフィッティング

40 Modeling snowline locations in protostars: The impact of the structure of protostellar cloud cores

Nadia M. Murillo, Tien-Hao Hsieh, Catherine Walsh ★ Abridged Context: Snowlines during star and disk formation are responsible for a range of effects during the evolution of protostars, such as setting the chemical composition of the envelope and disk. This in turn influences the formation of planets by changing the elemental compositions of solids and affecting the collisional properties and outcomes of dust grains. Snowlines can also reveal accretion bursts, providing insight into the formation process of stars. Methods: A numerical chemical network coupled with a grid of cylindrical-symmetric physical models was used to identify what physical parameters alter the CO and H_2O snowline locations. The investigated parameters are the initial molecular abundances, binding energies of CO and H_2O, heating source, cloud core density, outflow cavity opening angle, and disk geometry. Simulated molecular line emission maps were used to quantify the change in the snowline location with each parameter. Conclusions: The models presented in this work show that the CO and H_2O snowline locations do not occur at a single, well-defined temperature as is commonly assumed. Instead, the snowline position depends on luminosity, cloud core density, and whether a disk is present or not. Inclination and spatial resolution affect the observability and successful measurement of snowline locations. We note that N_2H^+ and HCO^+ emission serve as good observational tracers of CO and H_2O snowline locations. However, constraints on whether or not a disk is present, the observation of additional molecular tracers, and estimating envelope density will help in accurately determining the cause of the observed snowline position. Plots of the N_2H^+ and HCO^+ peak emission radius versus luminosity are provided to compare the models with observations of deeply embedded protostars aiming to measure the CO and H_2O snowline locations.

41 ALMA Images the Eccentric HD 53143 Debris Disk

Meredith A. MacGregor, Spencer A. Hurt, Christopher C. Stark, Ward S. Howard, Alycia J. Weinberger, Bin Ren, Glenn Schneider, Elodie Choquet, Dmitri Mawet ★ We present ALMA 1.3 mm observations of the HD 53143 debris disk - the first infrared or millimeter image produced of this 1 Gyr-old solar-analogue. Previous HST STIS coronagraphic imaging did not detect flux along the minor axis of the disk which could suggest a face-on geometry with two 'clumps' of dust. These ALMA observations reveal a disk with a strikingly different structure. In order to fit models to the millimeter visibilities and constrain the uncertainties on the disk parameters, we adopt an MCMC approach. This is the most eccentric debris disk observed to date with a forced eccentricity of 0.21 ± 0.02, nearly twice that of the Fomalhaut debris disk, and also displays apocenter glow. Although this eccentric model fits the outer debris disk well, there are significant interior residuals remaining that may suggest a possible edge-on inner disk, which remains unresolved in these observations. Combined with the observed structure difference between HST and ALMA, these results suggest a potential previous scattering event or dynamical instability in this system. We also note that the stellar flux changes considerably over the course of our observations, suggesting flaring at millimeter wavelengths. Using simultaneous TESS observations, we determine the stellar rotation period to be 9.6 ± 0.1 days.

1Gyr(10億歳)のデブリディスクのALMA観測
距離18.3 pc (GAIA)

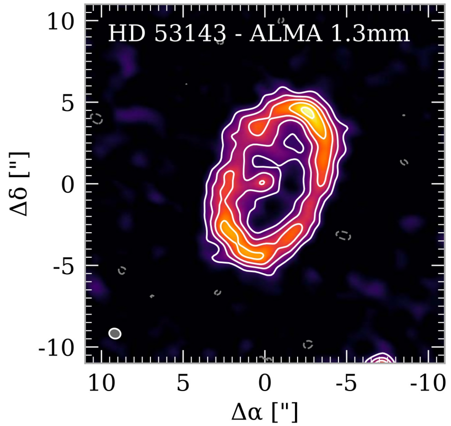

Figure 1. The first millimeter image of HD 53143 taken with ALMA shows an asymmetric distribution of dust with a bright point source in the center coincident with the star. Contours are in steps of 3σ ($3\times$ the rms noise of 5.6 μJy beam^{-1}). The gray ellipse in the lower-left corner indicates the $1''.13 \times 0''.92$ synthesized beam with natural weighting.

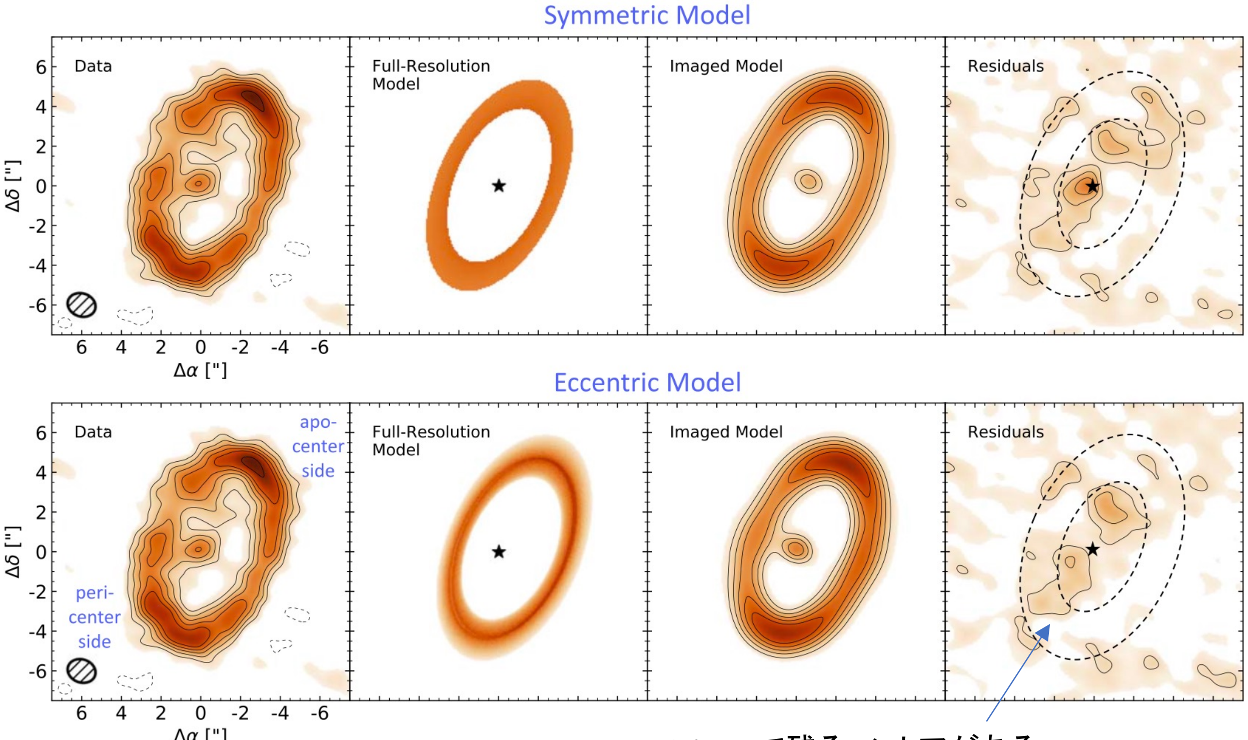

6sigmaで残るコントアがある
inner disk の追加の構造？
それとも外側の円盤から内側に来ている成分？

Eccentric modelがよくfitできる

・Forced eccentricity 0.21

・Proper eccentricity 0.11

=>フォーマルハウトよりも大きい
デブリ円盤の中では最も大きい

TESSで同じ期間に観測していた
ミリ波の増光はフレアか？

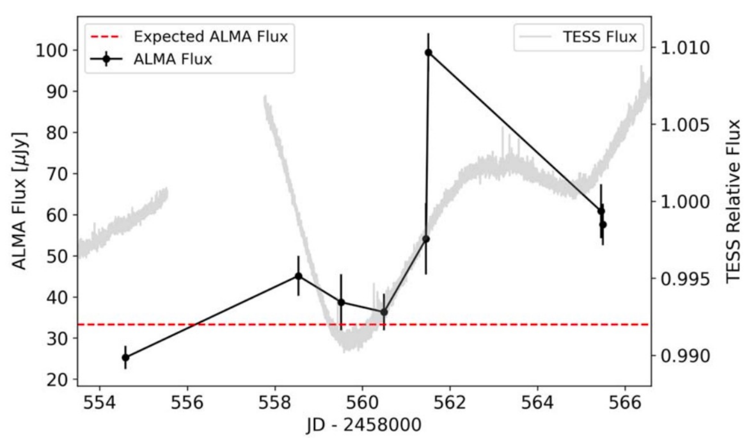

Figure 3. The flux density of the central star varies over the course of our eight ALMA observations, indicating potential flaring. Each point in this light curve represents the best-fit stellar flux density in each individual observation. For reference, the expected photospheric flux of 33 μJy for a G9V star is indicated by the dashed red line. Simultaneous TESS observations plotted in gray indicate significant spot modulation.

42 **Unraveling the observational signatures of cloud-cloud collision and hub-filament systems in W31**

A. K. Maity, L. K. Dewangan, H. Sano, K. Tachihara, Y. Fukui, N. K. Bhadari ★ To understand the formation process of massive stars, we present a multi-scale and multi-wavelength study of the W31 complex hosting two extended HII regions (i.e., G10.30-0.15 (hereafter, W31-N) and G10.15-0.34 (hereafter, W31-S)) powered by a cluster of O-type stars. Several Class I protostars and a total of 49 ATLASGAL 870 μm dust clumps (at d = 3.55 kpc) are found toward the HII regions where some of the clumps are associated with the molecular outflow activity. These results confirm the existence of a single physical system hosting the early phases of star formation. The Herschel 250 μm continuum map shows the presence of hub-filament system (HFS) toward both W31-N and W31-S. The central hubs harbour HII regions and they are depicted with extended structures (with $T_d \sim$ 25-32 K) in the Herschel temperature map. In the direction of W31-S, an analysis of the NANTEN2 ^{12}CO(J = 1-0) and SEDIGISM ^{13}CO(J = 2-1) line data supports the presence of two cloud components around 8 and 16 km s^{-1}, and their connection in velocity space. A spatial complementary distribution between the two cloud components is also investigated toward W31-S, where the signposts of star formation, including massive O-type stars, are concentrated. These findings favor the applicability of cloud-cloud collision (CCC) around ~2 Myr ago in W31-S. Overall, our observational findings support the theoretical scenario of CCC in W31, which explains the formation of massive stars and the existence of HFSs.

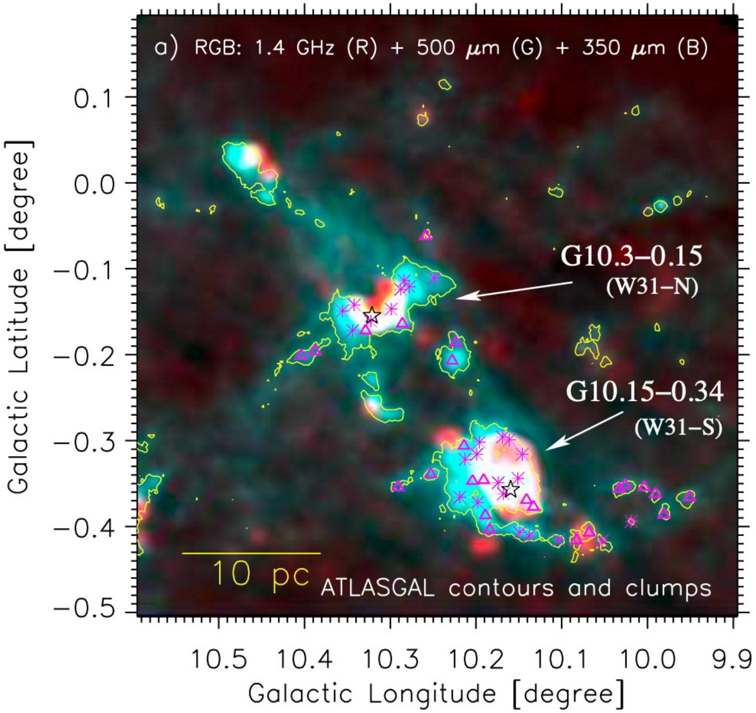

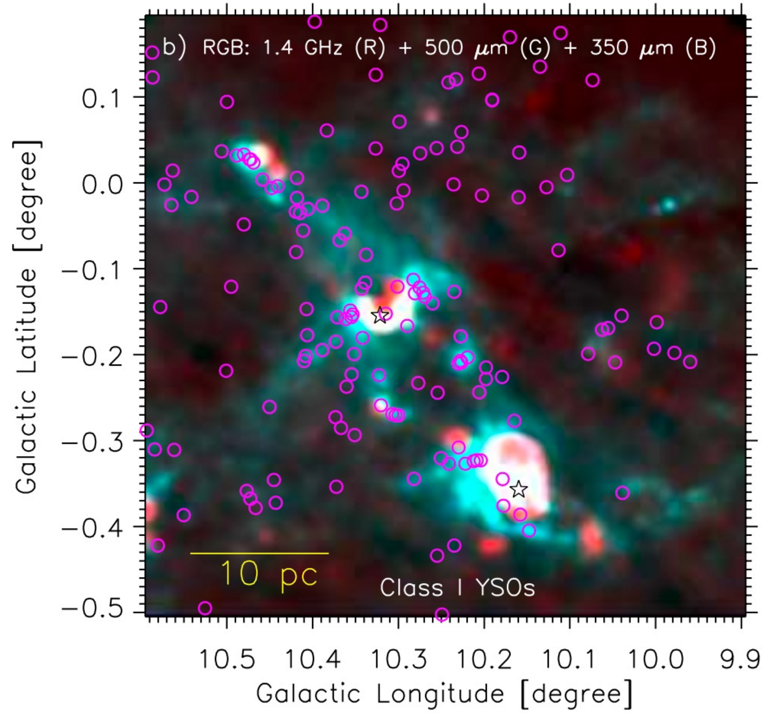

◯: Class I ソース

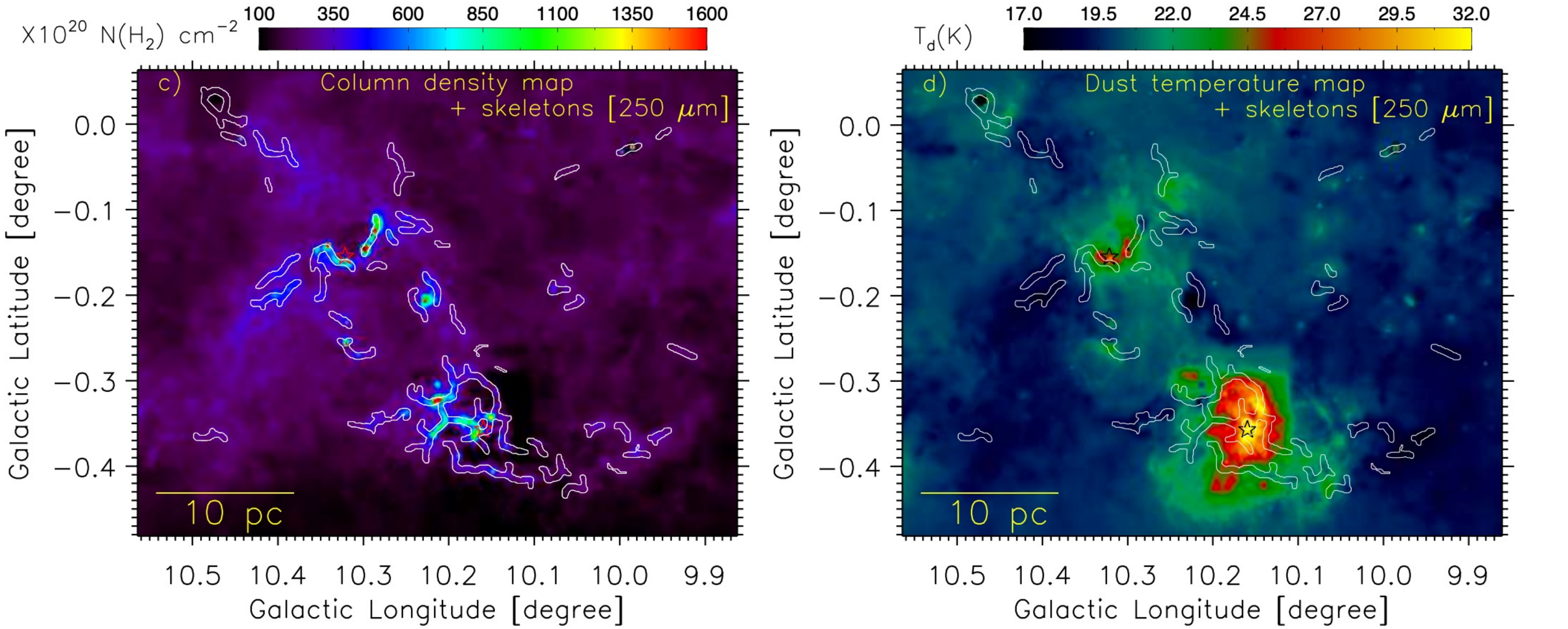

*フィラメントの同定はgetsf(Men’shchikov 2021)というアルゴリズムを使用

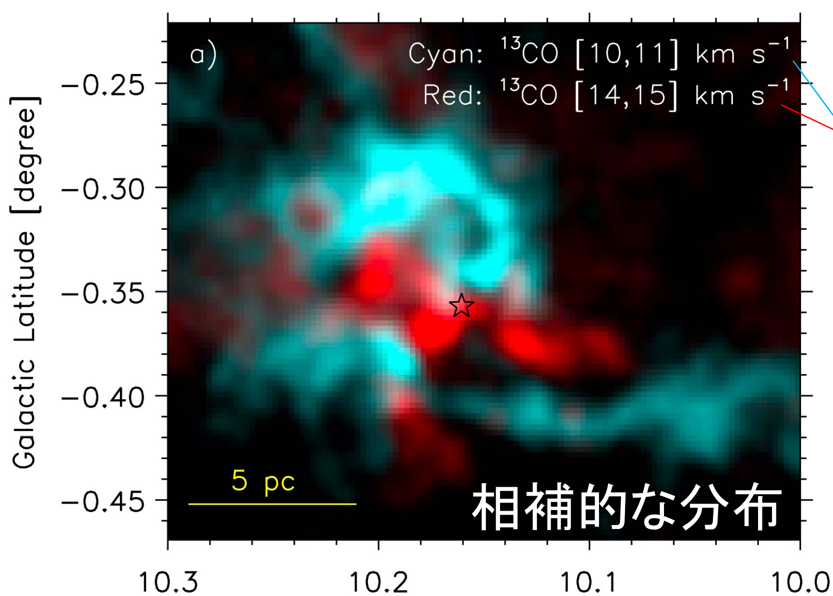

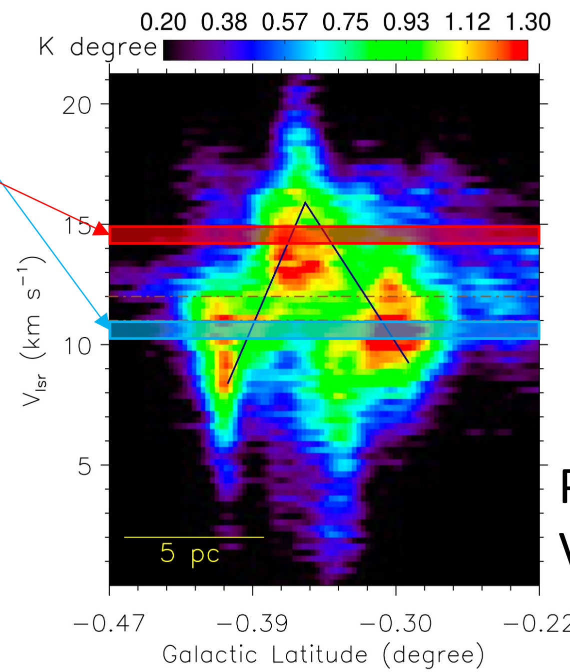

PV図上の
V-型構造

表示の画像

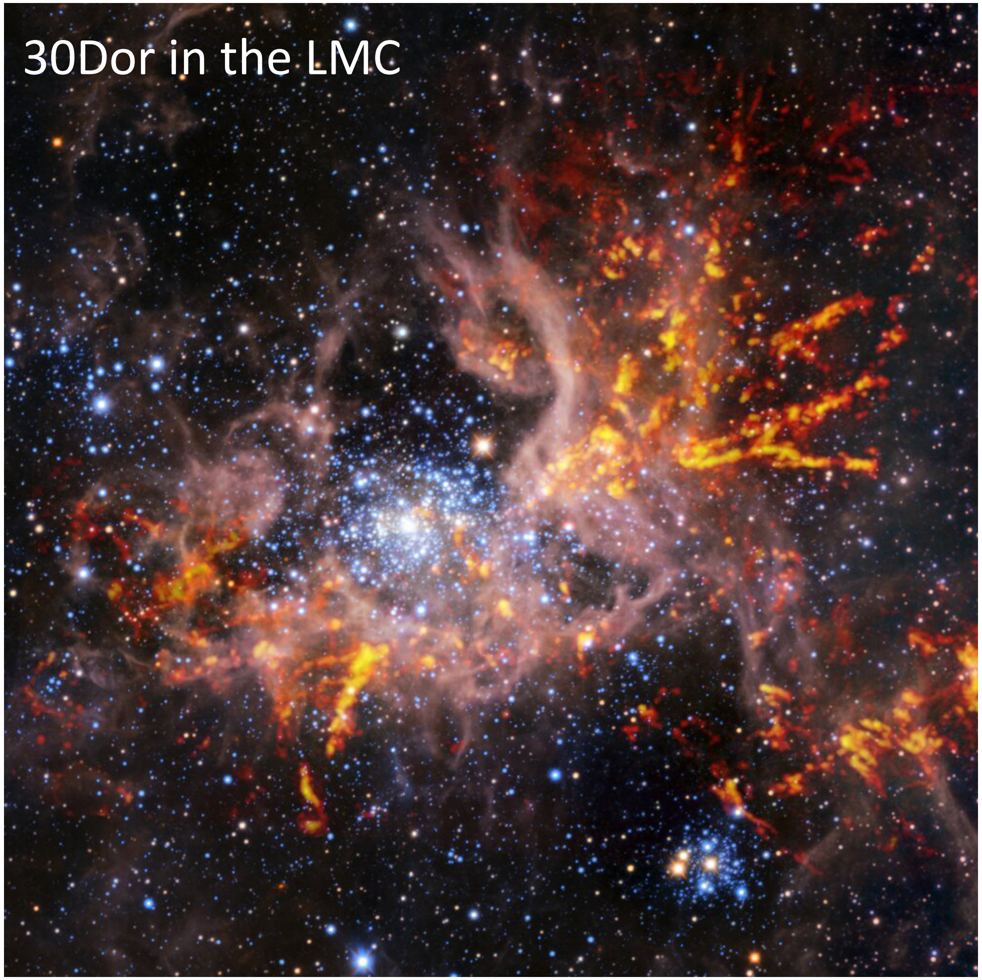

The bright red-yellow streaks superimposed on the background NIR image come from CO observations taken by ALMA, revealing complex filamentary networks stretching away approximately, from the central cluster, not unlike an upscaled version of the Orion Nebula Cluster. Credit: ESO, ALMA (ESO/NAOJ/NRAO)/Wong et al. 2022, ESO/M.-R. Cioni/VISTA Magellanic Cloud survey.

共同研究者(Tony Wong+22)と自身の貢献の宣伝
大型の扇型フィラメント構造がLMCで見つかりつつある
(Tokuda+22及び、Fukui+19: Tokuda+19も参照)